



ISSN: 0067-2904

## Effect of Biosynthesis ZnO-NPs on Renal Injury Caused by Hydrogen Peroxide in Adults Male Rats

Masar J. AL-Kurdy, Meraim A. Kazaal

Nursing techniques department, Technical Institute of Al-Diwaniyah, AL-Furat AL- Awsat Technical University, Iraq

Received: 19/5/2024    Accepted: 25/11/2024    Published: 30/12/2025

### Abstract

Nanoparticles produced through biological synthesis have shown significant potential in various therapeutic applications. This study was designed to explore the potential of biosynthesized zinc oxide nanoparticles (ZnO-NPs) in alleviating kidney disorders, which are among the most prevalent health issues globally. The study included the preparation of ZnO-NPs using black currant extract. The ZnONPs were formed by dissolving black currant in a zinc oxide solution with pH adjusted to 12. During the mixing process, Zinc acetate dehydrate was reduced to ZnONPs, resulting in a color change of the solution from white to pale yellow color within a few minutes. The synthesized ZnONPs were separated by centrifugation (4000rpm/ 5min), characterized by x-ray diffraction (XRD), Scanning Electron Microscopy (SEM) Fourier Transmission Infrared Spectroscopy (FT-IR) methods. The effectiveness of these particles was tested on adult male rats whose kidney disorders were induced by H<sub>2</sub>O<sub>2</sub>. The adult male rats were divided into four groups based on their dosage: the first (G1) received 0.5% H<sub>2</sub>O<sub>2</sub>, the second (G2) received 0.5% H<sub>2</sub>O<sub>2</sub> and ZnO-NPs (10 µg /kg), and the third group received ZnO-NPs (10 µg /kg). They were mixed along with the control group, which only got distilled water. The findings indicated that G1 had the highest levels of bilirubin, creatinine, and urea nitrogen at rates of 66.15, 44.46, and 4.60 µmol/l, respectively. In contrast, G2 showed levels of 45.52, 36.79, and 2.27 µmol/l, respectively, and G3 had rates of 41.41, 34.38, and 1.33 µmol/l, respectively. A high concentration of Malondialdehyde (MDA) was detected in group G1 (14.30 µmol/l), a lower concentration in group G2 (9.91 µmol/l), and the lowest concentration of MDA in group G3 (6.59 µmol/l), which was close to the control group (6.55 µmol/l). As well as found significant changes in MDA concentrations between groups G1 and G3 or control. Glutathione peroxidase (GPX) levels dropped in group G1 (2.26 µmol/l) but rose in groups G3 (4.72 µmol/l) and control (4.68 µmol/l). Histologically, the animals treated with both control and ZnO-NPs had similar approximate kidney structures, characterized by regular renal tubules and glomeruli. However, sections of the kidneys of H<sub>2</sub>O<sub>2</sub>-treated rats were inspected under a microscope, and necrotized glomeruli, atrophic glomeruli, and renal tubular epithelial necrosis were seen. The cortex of the ZnO-NPs treated group G2 was normal, but the glomeruli and some tubules had been largely damaged. Our results suggest that ZnO-NPs play a beneficial role in mitigating the harmful effects of H<sub>2</sub>O<sub>2</sub>-induced kidney damage in rats. Where ZnO-NPs can be considered as an antioxidant, and protective agent against kidney injury and cytoprotective activity.

**Keywords:** Biosynthesis ZnONPs, Bilirubin, Creatinine, Urea nitrogen, MDA, GPX

\*Email: [dw.msr@atu.edu.iq](mailto:dw.msr@atu.edu.iq)

## تأثير التخليق الحيوي لـ $ZnO-NPs$ على الإصابة الكلوية الناجمة عن بيروكسيد الهيدروجين في ذكور الجرذان البالغة

مسار جبار جري الكردي\*، مريم عطية خزل

قسم تقنيات التمريض ، المعهد التقني الديوانية ، جامعة الفرات الأوسط التقنية ، العراق

### الخلاصة

اظهرت الجسيمات النانوية المصنعة حيويًا امكانيات كبيرة في تطبيقات علاجية مختلفة. صُممت هذه الدراسة لاستكشاف امكانية جزيئات اكسيد الزنك النانوية المصنعة بايولوجيا في تخفيف اضطرابات الكلى والتي تعد حاليًا واحدة من أكثر المشاكل الصحية شيوعًا على مستوى العالم. تضمنت دراستنا تحضير جسيمات نانوية من أكسيد الزنك باستخدام مستخلص الزبيب الأسود، تم تكوين جسيمات أكسيد الزنك النانوية من خلال إذابة الزبيب الأسود في محلول أكسيد الزنك بدرجة حموضة معدلة الى 12. اثناء عملية الخلط، تم اختزل أسيتات الزنك إلى جسيمات أكسيد الزنك النانوية مما أدى الى تغير لون المحلول من الأبيض إلى اللون الأصفر الباهت في غضون بضع دقائق. تم فصل جسيمات أكسيد الزنك النانوية المحضرة بواسطة الطرد المركزي (4000 دورة في الدقيقة / 5 دقائق)، وتم تميزها باستخدام حيود الأشعة السينية (XRD) والمجهر الإلكتروني الماسح (SEM) وطيف الأشعة تحت الحمراء (FT-IR). وتم اختبار فعالية هذه الجزيئات على ذكور الجرذان البالغة التي استحدثت اضطرابات الكلى عن طريق بيروكسيد الهيدروجين. تم تقسيم الحيوانات إلى أربع مجموعات بالاعتماد على جرعاتها: المجموعة الأولى (G1) جرعت بيروكسيد الهيدروجين 0.5%، والثانية (G2) جرعت بيروكسيد الهيدروجين 0.5% و جسيمات اكسيد الزنك النانويه (10 ميكروجرام/كجم)، والمجموعة الثالثة (G3) جرعت جسيمات اكسيد الزنك النانويه (10 ميكروجرام/كجم). تم خلطهم مع مجموعة السيطرة، التي جرعت الماء المقطر فقط. اشارت النتائج أن G1 كان لديه أعلى مستويات من المادة الصفراء (البيليروبين) والكرياتينين ونيتروجين يوريا بمعدلات 66.15، 44.46، و4.60 ميكرومول/لتر، على التوالي، في المقابل اظهرت المجموعة G2 مستويات 45.52، 36.79، و2.27 ميكرومول/لتر، على التوالي. وG3 كانت معدلاتها 41.41 و34.38 و1.33 ميكرومول/لتر على التوالي. وجدت تركيزًا عاليًا من المالونديالدهيد في المجموعة G1 (14.30 ميكرومول/لتر)، وتركيزًا أقل في المجموعة G2 (9.91 ميكرومول/لتر)، وأدنى تركيز المالونديالدهيد في المجموعة G3 (6.59 ميكرومول/لتر)، والذي كان قريبًا من المجموعة الضابطة (6.55 ميكرومول/لتر). لقد وجدنا أيضًا تغييرات كبيرة في تركيزات المالونديالدهيد بين المجموعتين G1 وG3 و السيطرة. انخفضت مستويات الجلوتاثيون بيروكسيداز في المجموعة G1 (2.26 ميكرومول/لتر)، لكنها ارتفعت في المجموعتين G3 (4.72 ميكرومول/لتر) ومجموعة السيطرة (4.68 ميكرومول/لتر). نسيجيًا، كان لدى حيوانات السيطرة والحيوانات المعالجة ب جسيمات اكسيد الزنك النانويه اظهرت تركيب الكلى متشابهة تقريبًا ، مع الأنابيب الكلوية والكبيبات الطبيعية ومع ذلك أجزاء من كلى الجرذان المعالجة بيروكسيد الهيدروجين فحصت تحت المجهر، والكبيبات النخرية، والكبيبات الضامرة، ونخر الظهارة الأنبوبية الكلوية تم مشاهدته . كانت قشرة المجموعة G2 المعالجة جسيمات اكسيد الزنك النانويه طبيعية، لكن الكبيبات وبعض الأنابيب تعرضت لأضرار كبيرة تشير نتائجنا الى ان جسيمات أكسيد الزنك النانوية تلعب دور مفيد في تقليل من التأثيرات الضارة لتلف الكلى التي يسببها بيروكسيد الهيدروجين في الجرذان، حيث يمكن اعتبار جسيمات أكسيد الزنك النانوية بمثابة مضاد للأكسدة وعامل وقائي ضد إصابة الكلى ونشاط المحمي للخلايا.

### 1. Introduction

The kidney is an essential organ responsible for waste elimination in the body and for regulating water and electrolyte balance [1]. Evaluation of some of the metabolic products

and pathological tissue wastes excreted by the kidneys provides important information about the health of this organ [2].

Renal damage poses a significant and complex clinical condition following kidney transplantation, renovascular operations, the excision of renal tumors, systemic hypotension, and resuscitation [3]. Numerous studies have demonstrated a clear link between ischemic kidney damage and increased morbidity in hospitalized patients. Renal injury causes acute tubular necrosis [4]. Through a complex inflammatory process marked by the generation of reactive oxygen species (ROS), heightened expression of inflammatory cytokines, infiltration of inflammatory cells, endothelial damage leading to necrotic tubular cell demise, and subsequent acute renal failure [5]. Despite remarkable advances in diagnostic technologies and therapy approaches, the management outcomes of ischemic kidney disorders remain unsatisfactory due to the heterogeneity of their underlying processes [6]. As a result, novel lines that target diverse pathogenic mechanisms such as oxidative stress, apoptosis, and inflammation are necessary to effectively address ischemic kidney disorders. [7]. Over the past decade, various treatment modalities have been explored for renal diseases including laser, herbal therapy, and the use of nanoparticles for certain metals such as gold, silver, and zinc [8].

The effect of zinc on biochemical and physiological processes has recently been the focus of considerable examination since zinc is an inevitable part of people, animals, plants, and microorganisms [9]. Moreover, more than 250 distinct enzymes, transcription factors, and biological gesture proteins include zinc. It is crucial for conserving the unity of the cell layer, straightening the manufacture of proteins, controlling the growth and distinction of cells, and bolstering the immune system [10].

Nanotechnology has facilitated the development of numerous useful nanoparticles (NPs). NPs have a large surface district and are very cell-reactive [11]. Zinc oxide nanoparticles (ZnO-NPs) are one of the many NPs being produced at present. Because of their high UV absorption, they are frequently found in sunscreen and cosmetics. Additionally, they are used in agriculture for fertilization, potential fungicidal properties, and cancer treatments [12,13]. ZnO-NPs also serve as preservatives and additives in the food and medical industries [12,13]. Zinc oxide nanoparticles, or ZnO-NPs, are extensively used in biomedicine, mainly as antibacterial and anticancer agents. This is accounted for by their strong capacity to source cell death, liberate zinc ions, and produce excess reactive oxygen species. ZnO-NPs have been shown in a recent study to possess anti-inflammatory, anti-oxidative stress, and anti-hyperglycemic effects in an animal model [12, 14]. This study investigates the impact of black currant-derived zinc oxide nanoparticles on oxidative stress and kidney dysfunction caused by exposure to H<sub>2</sub>O<sub>2</sub>.

## 2. Materials and methods

### 2.1. Extraction of Black currant

The black currant (*Vitis vinifera*) was sourced from a bazaar in AL-Diwaniya, Iraq, and was seedless. In Abu Ghraib/Baghdad, Iraq, the Ministry of Agriculture/Stat Board for Seed Testimony assessed black currants. Fluka, BDH, and Sigma-Aldrich supply all additional chemicals. One hundred grams of black currants were washed multiple times in distilled water, then dried at 40 C° in an incubator, and subsequently crushed in a blender. A solution of 10 g of black currant in 100 mL of distilled water was stirred for 10 to 20 min at 45 to 50 C° using a magnetic stirrer and hotplate and then left overnight at room temperature. Following this, the solution was centrifuged at 1000 rpm for 15 min, after the supernatant was separated and filtered using Whitman® filter paper No.4. Filtration and centrifugation processes were repeated two additional times [15].

## 2.2. Green Zinc Oxide Nanoparticle Synthesis and Characterization:

In this experiment, 0.25 g of zinc acetate dihydrate [ $\text{Zn}(\text{CH}_3\text{CO}_2)_2 \cdot 2\text{H}_2\text{O}$ ] (0.2 M) (Merck, Germany) was dissolved in 50 mL of deionized water. Subsequently, dropwise, 4 mL of the aqueous black currant was added while stirring for 10 min. The pH of the solution was raised to 12 by adding two moles of NaOH (BDH, England) dropwise while stirring. Afterwards, the precipitate was separated in a centrifuge at 4000 rpm for 15 minutes, and the resulting pellets were collected and washed twice with 70% ethyl alcohol, followed by deionized distilled water. The pellets were then dried at 60 °C to obtain the ZnO-NPs [16].

X-ray diffraction (Shemadzu-6000 Japan) was employed to identify the crystalline structure of amorphous ZnO-NPs. Additionally, Fourier-transform infrared spectroscopy (Shemadzu-8400s, Japan, 4000 - 400  $\text{cm}^{-1}$ ) was utilized to detect functional groups in black currants without seed (*Vitis vinifera*) and the produced nanoparticles. SEM (Tescan VegaII, Czech) was used to analyze the surface topography, size, and key composition of the ZnO-NPs. Furthermore, a 70% solution of  $\text{H}_2\text{O}_2$  (Sun-pharmacy/Iraq) was diluted with distilled water to create a 0.5%  $\text{H}_2\text{O}_2$  solution.

## 2.3. Renal injury induction

The present study examined the effectiveness of biologically synthesized zinc nanoparticles in the treatment of renal diseases by inflicting physiological damage on the kidneys of 32 adult male rats using  $\text{H}_2\text{O}_2$ .

## 2.4. Experiment with animal and study design

Adult male Sprague Dawley rats weighing 180-220 g were acquired from the College of Veterinary Medicine at the University of Baghdad in Iraq. Following approval from the ethics committee, ethics number: 118 on 16/3/2022), the rats were housed for 10 days following standard guidelines for the care and use of laboratory animals. The housing environment maintained a temperature range of 22-25 °C with a 12-hour light/dark cycle and a relative humidity of 50-70%. Rats were kept in clean polypropylene cages and provided with a steady supply of appropriate laboratory formula for food.

Three groups were added to the control group for the experiment. The dosage was as follows: one dose every day for four weeks:

- Control groups: 8 rats were orally supplemented with distilled water only
- G1: 8 rats were orally supplemented with distilled water containing 0.5% of  $\text{H}_2\text{O}_2$
- G2: 8 rats were orally supplemented with distilled water containing 0.5% of  $\text{H}_2\text{O}_2$  and ZnO-NPs (10  $\mu\text{g}/\text{kg}$ )
- G3: 8 rats were orally supplemented with ZnO-NPs (10  $\mu\text{g}/\text{kg}$  BW)

## 2.5. Samples collection

At the end of the experiment, all four groups of rats were anaesthetized using ether, and blood samples were collected by heart punctures in heparin-free tubes for use in biochemical and serological testing. Serum was separated from the coagulated blood samples by centrifugation at 300 RPM for 15 min. The serum samples were then transferred into Eppendorf-tubes and kept at -18°C until they were used.

## 2.6. Analyses of antioxidant and biochemical parameters

Serum creatinine, blood urea nitrogen, and total bilirubin were determined using enzymatic kits (Agappe, India). Malondialdehyde (MDA) and glutathione peroxidase (GPX) concentrations in serum were determined using an ELISA approach using enzymatic ELISA kits manufactured by Cohesion Bioscience (China).

## 2.7. Histological Preparation

Following standard histological protocols, kidney tissues designated for histopathological examination were fixed with 10% neutral-buffered formalin and embedded in paraffin. The paraffin was cut into sections of 4  $\mu\text{m}$  thickness using a microtome, and stained with hematoxylin and eosin (H&E) solution [17]. After staining, the tissues were subsequently mounted and coverslipped using a mounting medium and then examined microscopically (Olympus, Tokyo, Japan).

## 2.8. Statistics for analysis

All statistical results were given as mean and standard deviation (SD). The mean values were compared using one-way ANOVA, used with SPSS (SPSS Inc., Chicago, IL, USA) version 22 for Windows to determine the statistical significance between the groups. Differences were deemed significant when  $P < 0.05$  was reached [18].

## 3. Results

The green synthesis ZnO-NPs was achieved through the bioreduction of zinc acetate dehydrate through the utilization black currant aqueous extract as a reducing agent. The results of the current study indicated that the color changed from white to pale yellow after a few minutes results from the reaction of zinc acetate dehydrate with black currant extract. As depicted in Fig.1, the formation of the pale-yellow precipitate proceeded spontaneously for 8 hours at room temperature. Extending the incubation period, the rate of reduction and the production of ZnO-NPs may be enhanced. The pH and temperature of the reaction mixture are crucial controlling factors in nanoparticle biogenesis. Therefore, raising the pH to 12 facilitates the process and leads to an increase in weight of ZnO-NPs that are generated as the final product during the synthesis process, while lowering the pH produces purer ZnO-NPs.

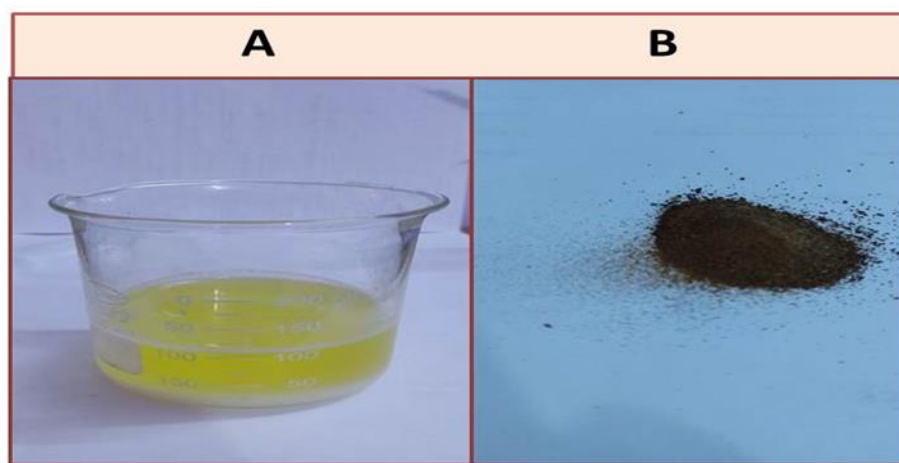


**Figure.1:** Image showed prepared of ZnO-NPs

(A) Pale yellow ZnO nanoparticles after mixing with Black currant. (B) ZnO nanopowder dried in an oven at  $60^{\circ}\text{C}$ .

## X-ray Diffraction (XRD):

The intensity of the diffracted rays is presented as a function of diffraction angles in the diffractogram of XRD ZnO-NPs Fig 2. X-ray diffraction peaks at theta angle-2 values of 30.98, 35.87, 47.26, 55.85, 61.93, 66.78, and 69.02 correspond to hkl values of (100), (002), (101), (102), (110), (103), (112), and (201) in our study, as illustrated in Fig. 2. The size of the nanoparticles was calculated using the Debye-Scherrer equation.

$$D = \frac{\kappa\lambda}{B \cos \theta} A^{\circ}$$

Where  $k$  is the structural factor, or Scherrer's constant (0.9), is the Bragg's diffraction point, is the XRD top full width at half most extreme, and  $D$  is the average size of glasslike molecules. Additionally, the average crystallographic size of the produced nanoparticles 50.13 nm was determined using Scherrer's formula. It was determined that the peaks corresponded to ICDD card number 01-079-0207. It was discovered that the nanoparticles had a hexagonal shape and that their lattice parameters,  $a$  ( $= b$ ), were 3.2568 5.2125 Å, where Å is the sum of Å and c. Tufts from the interaction between nano-plant extract.

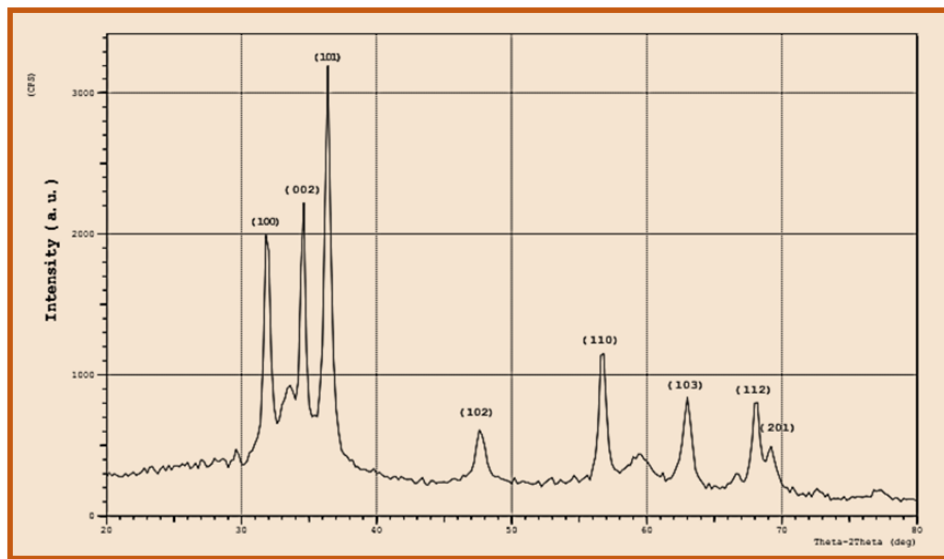


**Figure. 2:** X-ray diffraction pattern for of the Zinc oxide nanoparticles

### Scanning electron microscopy (SEM)

The SEM images taken at a magnification of 500 nm revealed crystal morphologies for ZnO-NPs generated from black currant extract. The green synthesis process of ZnO-NPs from Black Currant led to a closely packed periodic array of crystal structures. The differences in nanoparticle shape may be attributed to variations in size among the samples, allowing SEM to analyze only the particles on the surface of the sample. Furthermore, negative charges on the surface of nanoparticles contributed to their stability (measured by electrophoresis), whereas the soluble state prevents their aggregation by increasing electrostatic repulsion between particles (Fig 3).

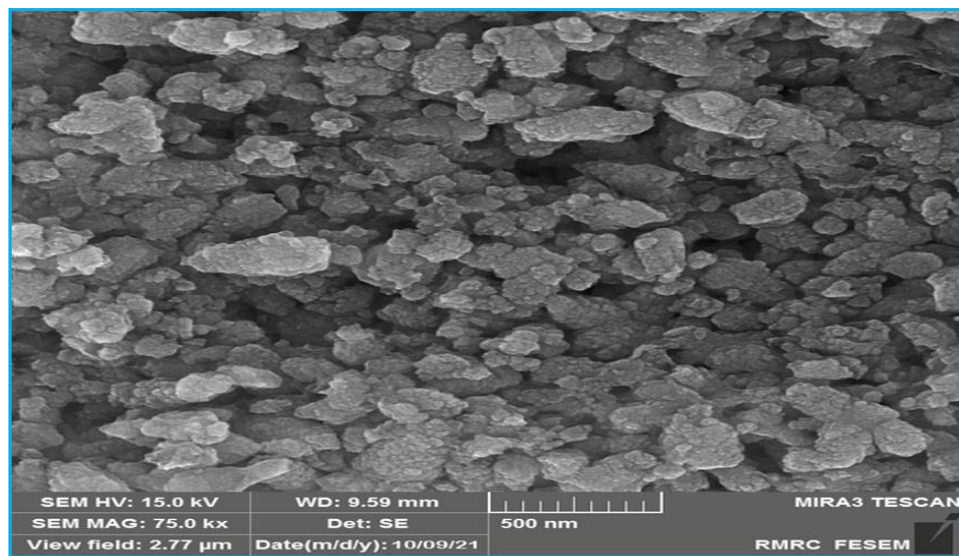


**Figure. 3:** SEM image (500nm) of the Zinc oxide nano-particles



### Fourier transform infrared spectroscopy (FTIR)

The peaks correspond to various functional groups that form in the final molecule. The bands observed at 3246, 2920, 1563, and 1324  $\text{cm}^{-1}$ , respectively, indicate the stretched frequencies of the OH, C-Haliph, C=C, and C-O bonds (this band was created as a result of nano-plant extract interaction). Additionally, the band at 480  $\text{cm}^{-1}$  represents the Zn-O bond, confirming the formation of nanoparticles, as illustrated in Figure 4.

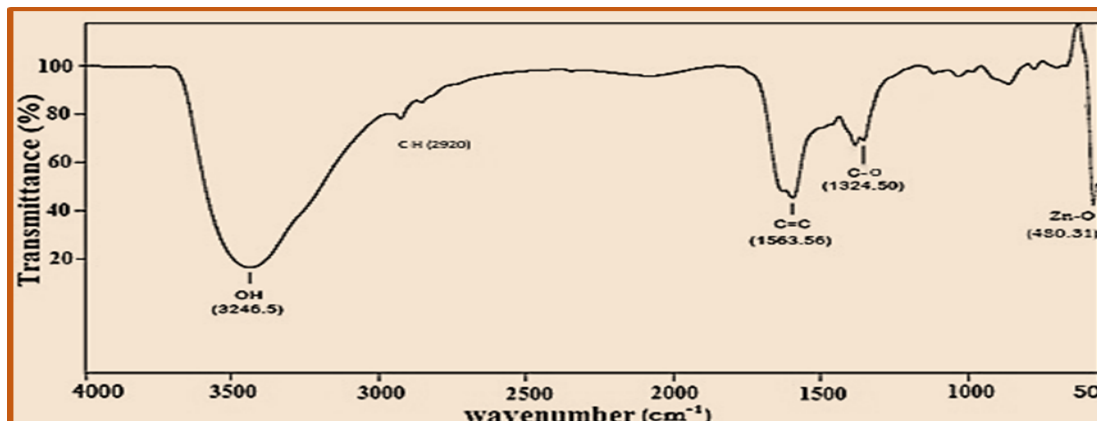


**Figure. 4:** FT-IR spectroscopy for the Zinc oxide nanoparticles

The results in Table (1) indicated a significant ( $P < 0.05$ ) elevation in bilirubin, creatinine, and urea nitrogen in the rats fed  $\text{H}_2\text{O}_2$  (group G1) at rates of 66.15, 44.46, and 4.60  $\mu\text{mol/l}$ , respectively as compared to other groups. The result also showed that G2 treated with  $\text{H}_2\text{O}_2$  and ZnONPs caused a significant decrease in this parameter at rates of 45.52, 36.79, and 2.27  $\mu\text{mol/l}$ . Furthermore, when comparing the findings of group G3 with the results of the control group, showed non-significant differences ( $P < 0.05$ ) in this parameter.

**Table 1:** Evaluation of some biochemical and antioxidant markers for experimental groups

Parameters	Control	G1	G2	G3	P value
	Mean $\pm$ SD	Mean $\pm$ SD	Mean $\pm$ SD	Mean $\pm$ SD	
Biochemical compounds ( $\mu\text{mol/l}$ )					
Bilirubin	41.33 $\pm$ 0.49	66.15 $\pm$ 2.66	45.52 $\pm$ 3.38	41.41 $\pm$ 0.84	0.053
Creatinine	34.44 $\pm$ 1.20	44.46 $\pm$ 1.28	36.79 $\pm$ 0.57	34.38 $\pm$ 1.30	0.237
Urea nitrogen	1.31 $\pm$ 0.17	4.60 $\pm$ 0.46	2.27 $\pm$ 0.37	1.33 $\pm$ 0.10	0.340
Oxidant -Antioxidants ( $\mu\text{mol/l}$ )					
MDA	6.55 $\pm$ 0.43	14.30 $\pm$ 0.38	9.91 $\pm$ 0.71	6.59 $\pm$ 0.54	0.097
GPX	4.68 $\pm$ 0.50	2.26 $\pm$ 0.21	4.11 $\pm$ 0.47	4.72 $\pm$ 0.28	0.300

The serum malondialdehyde (MDA) concentration exhibited a significant elevation ( $P < 0.05$ ) in the group treated with  $\text{H}_2\text{O}_2$  alone (G1) (14.30  $\mu\text{mol/l}$ ) compared to the value in the control G3. The results also showed that group G3 caused a significant decrease in this parameter compared to G1 and G2 treated groups, shown in Table (1). Conversely, the

concentration of GPX enzyme, on the other hand, decreased in group G1 (2.26  $\mu\text{mol/l}$ ), whereas it rose (4.72  $\mu\text{mol/l}$ ), (4.68  $\mu\text{mol/l}$ ) in groups G3 and control respectively.

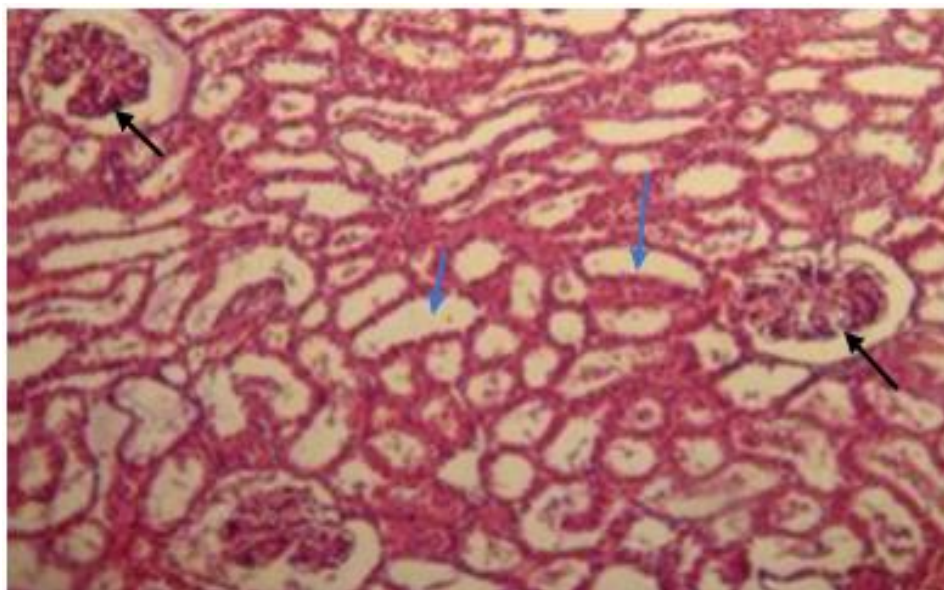


**Figure 5:** Histological section showed: normal renal cortex with normal glomeruli (black arrow) and renal tubules (blue arrow)(H&E stain; 40x)

Microscopic examination revealed a normal histological structure of Kidneys in the control group (Figure5). On the contrary, the microscopic examination of sections of kidneys of G1 treated group showed necrotized glomeruli, and renal tubular epithelial necrosis (Figure 6). The cortex of the ZnO-NPs treated group G2 was normal; however, some glomeruli and tubules had partial necrosis, as shown in Fig.7. Furthermore, the result of the group which is received ZnO-NPs showed normal glomeruli with normal renal cortex like control group exactly as shown in Figure 8.

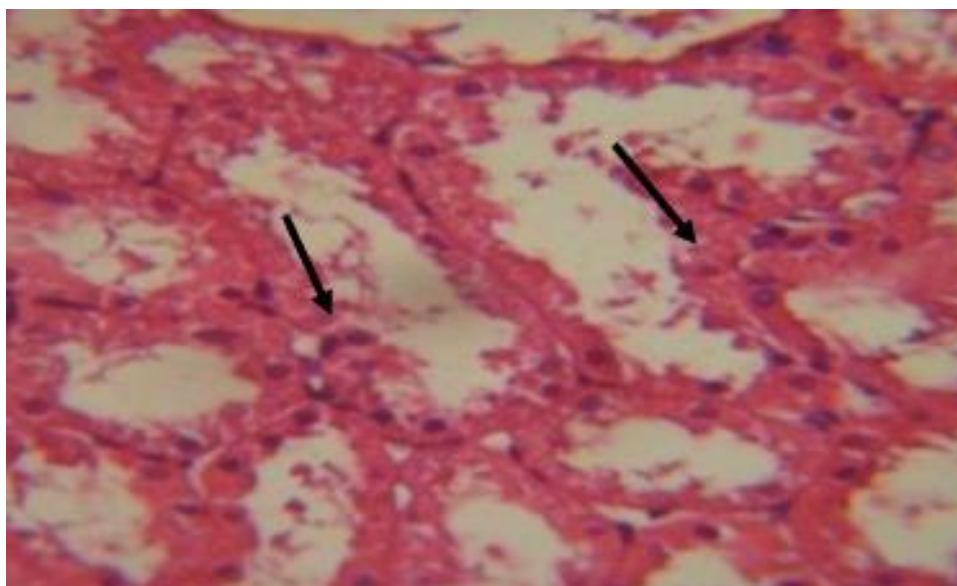


**Figure 6:** Histopathological section in kidney of G1 group showed: In cortex, necrotizing of proximal renal tubules (black arrow) (H&E stain 400x)



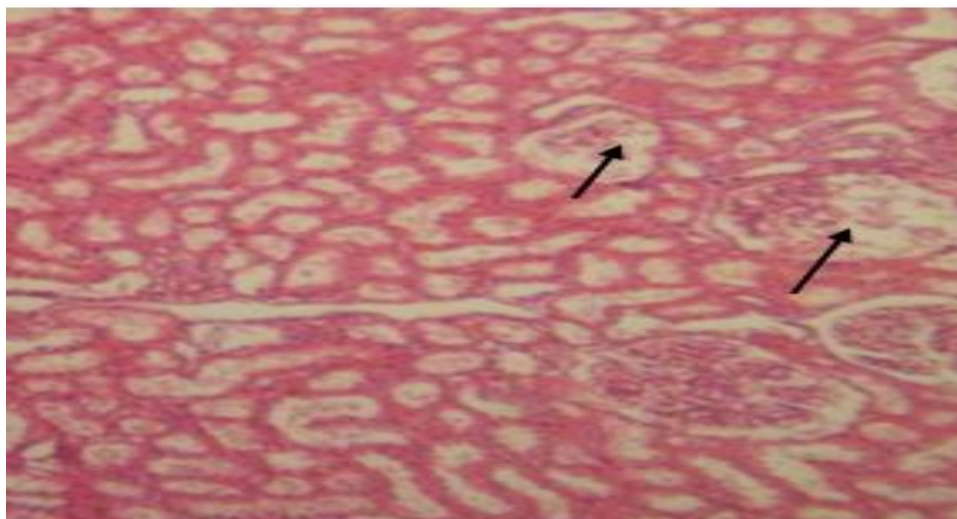


**Figure 7:** Histological section in kidney of G2 group showed: partial necrosis of glomeruli (black arrow) (H&E stain 40X)

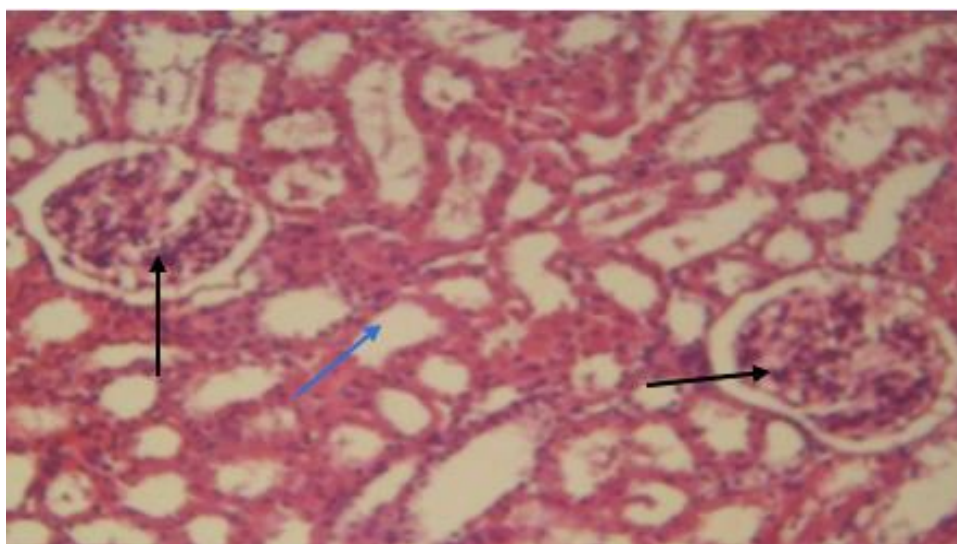


**Figure 8:** Histological section in kidney of G3 group showed: normal glomeruli with normal renal cortex (black arrow) and renal tubules (blue arrow) (H&E stain 400x)

#### 4. Discussion

Due to their tiny size, nanoparticles can travel to various organs and areas of the body after being consumed. After passing through the small intestine, they can enter the blood, brain, lung, heart, kidney, spleen, liver, intestine, and stomach [19]. Biodistribution studies have revealed that after being absorbed by the gastrointestinal system, tailored nanoparticles target the liver, kidneys, and spleen [20, 21].

The synthesis and characterization of ZnO NPs using black currant as a reducing agent resulted in a color change from white to pale-yellow color after mixing within a few minutes. Bio reduction involves reducing metal oxides or metal ions to zero valence metal nanoparticles which help phytochemicals like vitamins, polysaccharides, amino acids, polyphenolic compounds, terpenoids, and alkaloids, secreted from the plant [22]. According to the result of the XRD analysis conducted in the current study, the physical characteristic of particles in the prepared compound is crystallized nanoparticles with a mean average diameter of 50.13 nm. The XRD findings align with those of Hashemi [23] who present the XRD methods of ZnONPs synthesized by olive leaf extract. The green synthesis of ZnONPs using black currant extract showed hexagonal-amorphous NPs. ZnONPs

aggregation was prevented by organic compounds present in black currant extract leading to stabilized ZnO-NPs [24]. The current is in agreement with those reported by finding [25]. Fourier transform infrared spectroscopy (FTIR) measurements were employed to identify the functional groups present on the surface of biogenic ZnO-NPs [26]. The FTIR analysis of ZnO-NPs and biological material used in their synthesis (Black currant extract) demonstrated a change in the signal wave number  $\text{cm}^{-1}$  of the hydroxyl group when compared to biological extract with Zn-NPs. This suggests that -OH is involved in the production and stabilization of ZnO-NPs since it is employed in the zinc ion reduction and capping processes that result in ZnO-NPs, and that functional groups are present, exactly as in mushroom FTIR. These findings are compatible with previous research [27], which discovered functional groups in the plant extract recognized by high FTIR peaks in ZnO-NPs FTIR analysis, which are also consistent with the current study's FTIR results.

In this study, black currant zinc oxide nanoparticles demonstrated an effective role in reducing the damage caused by  $\text{H}_2\text{O}_2$  to the animals in group G2, and no toxic effect was found when administered alone to the animals in group G3, implying that these nano-particles may have an effective role in improving some kidney disorders or diseases by regulating the effectiveness of some antioxidant compounds and enzymes such as bilirubin and creatinine. Several studies have explored ZnO-NPs cellular activities, while other investigations have confirmed that specific nanoparticle concentrations are damaging to various critical functions [14,16].

The current findings are consistent with earlier research that has established the pharmacological effectiveness of Zn-ONPs in treating various histopathological illnesses such as cancer, inflammation, infertility, and others [13,14]. Furthermore, the results of this study were comparable with those of a recent work that aimed to evaluate the anticancer effectiveness of green biosynthesized Zn-NPs as a therapeutic intervention against kidney cancer induced in rats by ferric-nitrilotriacetate (Fe-NTA) [21].

The biochemical analysis revealed elevated levels of creatinine, bilirubin, MDA, and urea nitrogen in the G1 group treated with  $\text{H}_2\text{O}_2$ .  $\text{H}_2\text{O}_2$  is a key physiological component in the regulation of renal function, its plays a crucial role in Reactive Oxygen Species (ROS) intracellular signaling, serving as a mediator in various physiological processes. These include cell differentiation and proliferation, cellular metabolism, survival mechanisms, and immune response modulation. When  $\text{H}_2\text{O}_2$  increase in the kidney in some kinds of hypertension and diabetes, where it may play a role in renal injury [28]. In the G3-treated group, there were decreases in biochemical parameters and MDA concentration, along with an increase in GPX levels. Zinc has been shown to reduce oxidative stress and glutathione depletion, as well as to be engaged in all processes that protect cells by activating DNA repair, inhibiting apoptosis, and promoting cell proliferation [29]. Additionally, investigations have shown that ZnO-NP treatment decreased MDA concentration in a dose-dependent manner, the treatment lowered oxidative stress, protected cell membrane integrity from oxidative stress damage, and increased levels of antioxidant enzymes [30, 31]. The reduction in urea and keratin, as well as the increased activity of antioxidant enzymes like CAT and SOD, and the preservation of GSH content in renal tissue, could account for the ameliorative effect of ZnO-NPs on the histopathological changes seen in the ZnO -NPs-treated mice [32]. The generation of reactive oxygen species (ROS) and the consequent onset of oxidative stress were implicated in the decline of mitochondrial potential and lysosomal function [33]. According to the findings of research and other investigations. ZnO-NPs appear to have a short-term effect on renal function and tissues produced by oxidative stress after a single injection, especially at higher dosages (300 mg/kg). ZnO-NPs can catalyze the creation of

extremely reactive oxygen species such as hydrogen peroxide, hydroxyl radicals, and superoxide anions, all of which can injure bacterial or mammalian cells through oxidative damage [28, 34]. Additionally, studies have shown that ZnO nanoparticles can induce elevated levels of cytokines such as IFN- $\gamma$ , TNF- $\alpha$ , and IL-12, all of which play roles in immune cell differentiation and inflammatory responses. This disparity in results between our study and some previous studies may be due to the type of biological methods used to prepare ZnO-NPs, as well as the nanoparticle concentration used in the experiments, where previous experiments used high concentration doses of ZnO-NPs, such as 300 mg/kg, whereas our study used a low concentration (10  $\mu$ g /kg) [35,36].

The histological aspect of our investigation revealed that the kidney tissue of the G3 group of male rats treated with ZnO-NPs is identical to that of the control, but the rats treated with H<sub>2</sub>O<sub>2</sub> solely displayed necrosis and destruction. Also found a lower rate of kidney tissue damage in the G2 group, where giving ZnO-NPs in conjunction with H<sub>2</sub>O<sub>2</sub> played a role in reducing the kidney damage caused by H<sub>2</sub>O<sub>2</sub>, and this is consistent with the biochemical and antioxidant values mentioned in the previous section, indicating that the results were unified in determining the effect of the doses used on the efficacy and functioning of the kidney [35,36]

Previous research has highlighted the significant benefits of using nanoparticles [31,35] in the treatment of microbial infections, as it was demonstrated that when employed as an anti-inflammatory, these particles had a demonstrable impact in eliminating numerous harmful germs. Where our work adds to earlier studies is in the way of creating nanoparticles in an optimal concentration when employed as an antibacterial so that they do not have a detrimental impact on the organs of the body, particularly the liver and kidneys.

## Conclusion

The current study demonstrated that bio-synthesis ZnO-NPs from black currant extract can ameliorate dysfunction of kidneys induced by H<sub>2</sub>O<sub>2</sub> which causes many deleterious effects on the renal system such as a rise in serum urea, bilirubin and creatinine. This condition also induces oxidative stress in the body through elevation of MDA and decrease in GPX concentration and causes histopathological changes in the kidney.

## 6. Conflict of interest

Authors state that they have no competing of interests with any research or published work by other researchers in the same field of study.

## 7. Funding

Self-funded by authors.

## 8. Data availability

The datasets used and analyzed during the current study are available from the corresponding author on reasonable request.

## 9. Acknowledgment

The authors extend their heartfelt gratitude to the Deanship of Scientific Research at the Technical Institute of Al-Diwaniyah, AL-Furat AL Awsat Technical University, for their unwavering support.

## 10. Authors' contributions

MJA, and MAK were designed the experiments, and wrote the manuscript; JKA and MJA performed experiments and collected data, editing, and preparing the manuscript for journal submission. MJA, and MAK were checking the final approval of the version to be published. All authors read and approved the final manuscript.

## References

- [1] M. J. Al-Kurdy, "The effect of black currant selenium nanoparticles on dyslipidemia and oxidant-antioxidant status in D-galactose treated rats," *Kufa Journal For Veterinary Medical Sciences*, vol. 11, no. 1, pp. 23-38, 2020.
- [2] B. D. Humphreys, "Mechanisms of Renal Fibrosis," *Annu Rev Physiol*, vol. 10, no. 80, pp. 309-326, 2018.
- [3] M. Baradaran-Ghahfarokhi, "Radiation-induced kidney injury," *J Renal Inj Prev*, vol. 1, no. 2, pp. 49-50, 2012.
- [4] A. C. Webster, E.V. Nagler, R.L. Morton and P. Masson, "Chronic Kidney Disease," *Lancet*, vol. 389, no. 10075, pp. 1238-1252, 2017.
- [5] S. R. Mulay, A. Linkermann and H. J. Anders, "Necroinflammation in Kidney Disease," *J Am Soc Nephrol*, vol. 27, no. 1, pp. 27-39, 2016.
- [6] M. A. Hye Khan, B. Fish, G. Wahl, A. Sharma, J.R. Falck, M.P. Paudyal, J.E. Moulder, J.D. Imig and E.P. Cohen, "Epoxyeicosatrienoic acid analogue mitigates kidney injury in a rat model of radiation nephropathy," *Clin Sci (Lond)*, vol. 130, no. 8, pp. 587-99, 2016.
- [7] Y. Ma, F. Cai, Y. Li, J. Chen, F. Han and W. Lin, "A review of the application of nanoparticles in the diagnosis and treatment of chronic kidney disease," *Bioact Mater*, vol. 5, no. 3, pp. 732-743, 2020.
- [8] S. H. Lee, J.B. Lee, M.S. Bae, D.A. Balikov, A. Hwang, T.C. Boire, I.K. Kwon, H.J. Sung and J.W. Yang, "Current progress in nanotechnology applications for diagnosis and treatment of kidney diseases," *Adv Healthc Mater*, vol. 4, no. 13, pp. 2037-45, 2015.
- [9] H. H. Sandstead, "Zinc nutrition from discovery to global health impact," *Adv Nutr*, vol. 3, no. 5, pp. 718-9, 2012.
- [10] A.S. Prasad, "Discovery of human zinc deficiency: its impact on human health and disease," *Adv Nutr*, vol. 4, no. 2, pp. 176-90, 2013.
- [11] S. Mosleh-Shirazi, M. Abbasi, M.R. Moaddeli, A. Vaez, M. Shafiee, S.R. Kasaei, A.M. Amani and S. Hatam, "Nanotechnology Advances in the Detection and Treatment of Cancer," *An Overview. Nanotheranostics*, vol. 6, no. 4, pp. 400-423, 2022.
- [12] A. Król, P. Pomastowski, K. Rafińska, V. Railean-Plugaru and B. Buszewski, "Zinc oxide nanoparticles: Synthesis, antiseptic activity and toxicity mechanism," *Adv Colloid Interface Sci*, vol. 249, pp. 37-52, 2017.
- [13] M. J. Akhtar, M. Ahamed, S. Kumar, M.M. Khan, J. Ahmad and S.A. Alrokayan, "Zinc oxide nanoparticles selectively induce apoptosis in human cancer cells through reactive oxygen species," *Int J Nanomedicine*, vol. 7, pp. 845-57, 2012. <https://pubmed.ncbi.nlm.nih.gov/22393286/>
- [14] H. Mirzaei and M. Darroudi, "Zinc oxide nanoparticles: Biological synthesis and biomedical applications," *Ceram. Int*, vol. 43, pp. 907-914, 2017.
- [15] M.A. Awan, S. Akhter, A.U. Husna, M.S. Ansari, B.A. Rakha, A. Azam and S. Qadeer, "Antioxidant activity of Nigella sativa Seeds Aqueous Extract and its use for cryopreservation of buffalo spermatozoa," *Andrologia*, vol. 50, no. 6, pp. e13020, 2018.
- [16] T. Kaviyarasi, B. Muthulakshmi and C. Kavitha, "Green synthesis and characterization of zinc nanoparticle using Aegle marmelos leaf extract," *International Journal of ChemTech Research*, vol. 10, pp. 344-8, 2017.
- [17] J. F. Hillyer and R.M. Albrecht, "Gastrointestinal persorption and tissue distribution of differently sized colloidal gold nanoparticles," *J Pharm Sci*, vol. 90, no. 12, pp. 1927-36, 2001.
- [18] W. W. Daniel, C. L. Cross, "Biostatistics: a foundation for analysis in the health sciences. Wiley," 2018.
- [19] Y. Cui, H. Liu, M. Zhou, Y. Duan, N. Li, X. Gong, R. Hu, M. Hong and F. Hong, "Signaling

- pathway of inflammatory responses in the mouse liver caused by TiO<sub>2</sub> nanoparticles, " *J Biomed Mater Res A.*, vol. 96, no. 1, pp. 221-9, 2011.
- [21] M. Li, D. Lin and L. Zhu, "Effects of water chemistry on the dissolution of ZnO nanoparticles and their toxicity to *Escherichia coli*," *Environ Pollut*, vol. 173, pp. 97-102, 2013.
- [22] S. El-Sonbaty, E.I. Kandil and R.A. Haroun, "Assessment of the Antitumor Activity of Green Biosynthesized Zinc Nanoparticles as Therapeutic Agent Against Renal Cancer in Rats," *Biol Trace Elem Res.*, vol. 201, no. 1, pp. 272-281, 2023.
- [23] J. Qu, X. Yuan, X. Wang and P. Shao, "Zinc accumulation and synthesis of ZnO nanoparticles using *Physalis alkekengi* L.," *Environ Pollut.*, vol. 159 no.7, pp. 1783-1788, 2011.
- [24] S. Hashemi, Asrar, Z. and S. Pourseyedi. "Green synthesis of ZnO nanoparticles by olive (*Olea europaea*)". *Iet Nanobiotechnol*, vol. 10, pp.400-404, 2016.
- [25] D. Suresh, P.C. Nethravathi, H. Rajanaika, H. Nagabhushana, and S.C. Sharma, "Green synthesis of multifunctional zinc oxide (ZnO) nanoparticles using *Cassia fistula* plant extract and their photodegradative, antioxidant and antibacterial activities". *Materials Science in Semiconductor Processing*. vol. 31, pp. 446– 454, 2015.
- [26] F. Sultana, J. Barman, and M.C. Kalita, "Biogenic synthesis of ZnO Nanoparticles using *Polygonum chinense* leaf extract and their Antibacterial activity," *Int.J. of Nano. and App.*, vol. 11, no.2, pp. 155–165, 2017.
- [27] S. C. Singh and R. Gopal, "Zinc nanoparticles in solution by laser Ablation technique," *Bull Mater Sci*. vol. 30, pp. 291–293, 2007 .
- [28] Z. Salari, A. Ameri, H. Forootanfar, M. Adeli-Sardou, M. Jafari, M. Mehrabani and M. Shakibaie, "Microwave-assisted biosynthesis of zinc nanoparticles and their cytotoxic and antioxidant Activity," *J Trace Elem Med Biol.* , vol. 39, pp. 116–123, 2017
- [29] A. Noori, F. Karimi, S. Fatahian and F. Yazdani, "Effects of zinc oxide nanoparticles on renal function in mice," *International Journal of Biosciences*, vol. 5, pp. 140-146, 2014.
- [30] M. Afifi, O.A. Almaghrabi and N.M. Kadasa, "Ameliorative Effect of Zinc Oxide Nanoparticles on Antioxidants and Sperm Characteristics in Streptozotocin-Induced Diabetic Rat Testes," *Biomed Res Int*, pp. 153573, 2015.
- [31] A.I. Dawei, W. Zhisheng and Z. Anguo, "Protective effects of Nano-ZnO on the primary culture mice intestinal epithelial cells in vitro against oxidative injury," *J Anim Vet Adv.*, vol. 8, pp. 1964-7, 2009
- [32] J. Li, H. Chen, B. Wang, C. Cai, X. Yang, Z. Chai and W. Feng, "ZnO nanoparticles act as supportive therapy in DSS-induced ulcerative colitis in mice by maintaining gut homeostasis and activating Nrf2 signaling," *Sci Rep.* , vol. 7, pp. 43126, 2017
- [33] M.S. Mahmoud, R.B. Kassab and A. E. Moneim, "Zinc Oxide Nanoparticles Ameliorate Aluminum Chloride-Induced Hepato-Renal Oxidative Stress and Inflammation in Rats," *Int J Pharm Pharm Sci.*, vol. 12, pp. 11-20, 2020.
- [34] V.G. Reshma and P.V. Mohanan, "Cellular interactions of zinc oxide nanoparticles with human embryonic kidney (HEK 293) cells". *Colloids Surf B Biointerfaces*, vol. 157, pp. 182-190, 2017.
- [35] A. Adamcakova-Dodd, L.V. Stebounova, J.S. Kim, S.U. Vorrink, A.P. Ault, P.T. O'Shaughnessy, V.H. Grassian and P.S. Thorne, "Toxicity assessment of zinc oxide nanoparticles using sub-acute and sub-chronic murine inhalation models". *Part Fibre Toxicol*, vol. 11, pp. 15, 2014.
- [36] M.A. Kazaal, M.S. Kadhim and A. Y. Othman, "Effect of Different Biosynthesis Methods for Silver Nanoparticles on Their Anti-bacterial Activity". *Turkish Journal of Physiotherapy and Rehabilitation*, vol. 32, pp. 11527-11536, 2021.
- [37] C. Hanley, A. Thurber, C. Hanna, A. Punnoose, J. Zhang and D.G. Wingett, "The influences of cell type and ZnO nanoparticle size on immune cell. Cytotoxicity and cytokine induction," *Nanoscale. Research Letters*, vol. 4, pp. 1409-20, 2009. <https://doi.org/10.1007%2Fs11671-009-9413-8>